AD-A113 478 NAVAL OCEAN RESEARCH AND DEVELOPMENT ACTIVITY NSTL S--ETC F/G 11/9
HYDRODYNAMIC TEST AND EVALUATION OF A NEWLY DEVELOPED KEVLAR RO--ETC(U)
FEB 82 D A MILBURN, P RISPIN

UNCLASSIFIED NORDA-TN-118 NL

END
DATE FILMED
5 82
DTIC

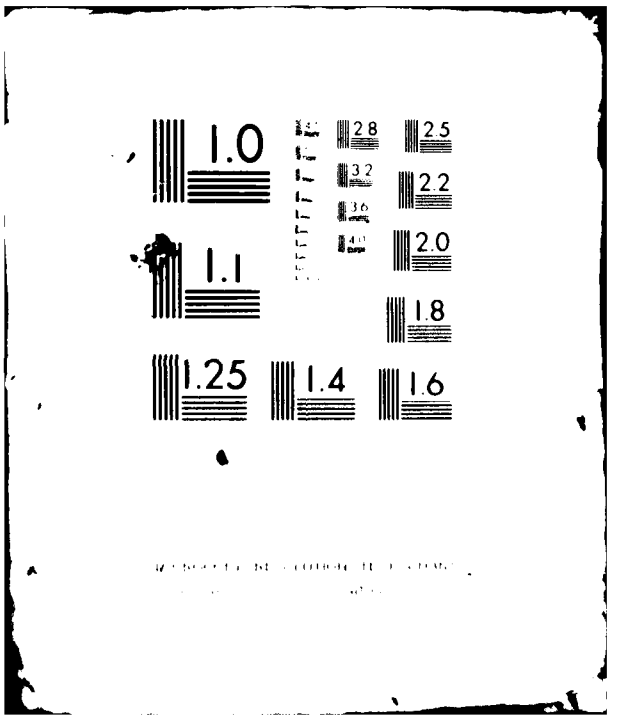
1.0
1.1
1.25
1.4
1.6
2.8
3.2
3.6
4.0
2.5
2.2
2.0
1.8

NORDA Technical Note 118

Hydrodynamic Test and Evaluation of a Newly Developed Kevlar Rope Fairing

Naval Ocean Research and Development Activity
NSTL Station, Mississippi 39529

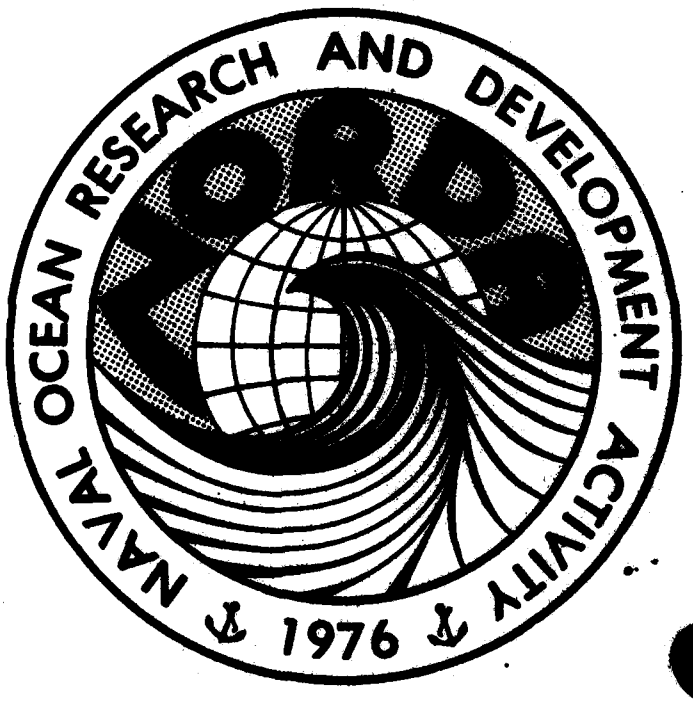

Darrell A. Milburn
*Paul Rispin

Ocean Science and Technology Laboratory
Ocean Technology Division

(*David W. Taylor Naval Ship Research and Development Center)

December 1981

ABSTRACT

The strumming and drag performance of a newly developed Kevlar rope fairing have been determined experimentally. In one experiment, faired and unfaired rope samples of the same diameter were towed with one end free to obtain their normal and tangential drag coefficients. Results of the experiment are plotted versus Reynolds number and show that the fairing increases cable drag substantially. In another experiment the same ropes were also towed with a heavy, streamlined body attached. By comparing their resonantly excited tension fluctuations, it is found that the fairing reduces flow-induced cable vibrations.

CONTENTS

LIST OF ILLUSTRATIONS		iv
LIST OF TABLES		iv
NOTATION		v
I.	INTRODUCTION	1
II.	DRAG EXPERIMENTS	1
	A. Towing Theory	1
	B. Sensitivity Analysis	6
	C. Experimental Setup and Procedures	9
	D. Measurements and Observations	10
	E. Drag Coefficient Comparisons	14
III.	STRUMMING EXPERIMENT	16
	A. Vibration Theory for Taut Cables	16
	B. Experimental Setup and Procedures	18
	C. Discussion of Results	19
IV.	CONCLUSIONS	19
V.	REFERENCES	22

ILLUSTRATIONS

Figure 1.	Various types of cable fairings	2
Figure 2.	Photograph of Kevlar rope samples	3
Figure 3.	Free-body diagram of tow cable element	4
Figure 4.	Sensitivity relation coefficients versus towing angle	8
Figure 5.	Schematic of experimental setup for cable drag measurements	9
Figure 6.	Photographs of 6.1 m long rope samples towed freely at various speeds	11
Figure 7.	Normal drag coefficients versus Reynolds number	15
Figure 8.	Tangential drag coefficients versus Reynolds number	17
Figure 9.	Schematic of experimental setup for cable strumming measurements	18
Figure 10.	Tension fluctuation data for the rope samples	20
Figure 11.	Vibration characteristics of the bare rope sample	21

TABLES

Table 1.	Measured Rope Sample Characteristics	12
Table 2.	Cable Drag Measurements	12
Table 3.	Normal Drag Coefficient and Reynolds Number as a Function of Tow Speed	13
Table 4.	Tangential Drag Coefficient and Reynolds Number as a Function of Tow Speed	14

NOTATION

C_n	Normal drag coefficient of cable
C_t	Tangential drag coefficient of cable
d	Cable diameter
EA	Modulus of rigidity
f_k	Natural frequency of a taut string
f_s	Vortex shedding frequency
F_n	Normal hydrodynamic force per unit cable length
F_t	Tangential hydrodynamic force per unit cable length
k	Vibration mode number
L	Cable length
M	Virtual mass per unit length of cable
R_n	Reynolds number for normal flow
R_t	Reynolds number for tangential flow
s	Distance along cable
S	Strouhal number
t	Time
T	Cable tension
T_l	Static or mean cable tension at tow point, s = L
T_a	Amplitude of fluctuating tension, T_f
T_f	Tension fluctuation
V	Towing or relative fluid flow speed
w	Weight per unit length of cable in fluid
Y	Strumming displacement amplitude
ν (nu)	Kinematic viscosity
ϕ (phi)	Angle between tow direction and cable tangent vector

ϕ_c Critical towing angle

ρ(rho) Fluid density

ω(omega) Frequency of tension fluctuations

I. INTRODUCTION

Marine cables exposed to ocean currents are subject to periodic transverse and longitudinal motions caused by vortex-induced forces. This phenomenon, called strumming, can lead to reduced cable fatigue life, increased cable drag, and measurement errors from attached sensors -- especially acoustic types. Experimentally, it is well-known that strumming can be reduced by attaching devices to the cable, Griffin et al. (1981). This, in turn, has led to the development of various types of devices over the years. Some examples, which are more commonly referred to as fairings, are shown in Figure 1. A hydrodynamic evaluation of these and other types of fairings is given by Vandiver and Pham (1977) and Rispin et al. (1977).

A more recently developed fairing is shown and described in Figure 2. The fairing was specifically developed for small diameter Kevlar ropes (less than 25 mm) and is less expensive than the other viable choices available. And this makes it a good candidate for the Kevlar ropes and cables that comprise most of the moored systems being developed at the Naval Ocean Research and Development Activity.

To answer the question about its hydrodynamic performance, two experiments were conducted in the high speed tow basin at the David Taylor Naval Ship Research and Development Center. The objectives of the experiments were to determine to what extent the fairing reduces strumming and to measure the effect of the fairing on the normal and tangential drag coefficients of the rope. Two 30.8 m long rope samples were available for the experiments: One was faired, the other was not. A short length of each is shown in the photograph of Figure 2.

The results of the experiments conducted on the two rope samples are contained herein. Presentations also include the theoretical basis of each experiment and a description of the experimental setup and procedures.

II. DRAG EXPERIMENTS

A. TOWING THEORY

The cable drag experiment is based on a two-dimensional, steady-state model of a cable subjected to a relative fluid flow. The model, as developed by Pode (1951), assumes that all forces and the cable are coplanar. It further assumes that the flow is constant and uniform with depth, and that the cable is inextensible and perfectly flexible.

The forces acting on an arbitrary cable element of infinitesimal length, ds, are shown in the free-body diagram of Figure 3 where the following notation is used:

$w\,ds$ = weight of cable element in water

T = cable tension

$F_n\,ds$ = normal component of hydrodynamic force

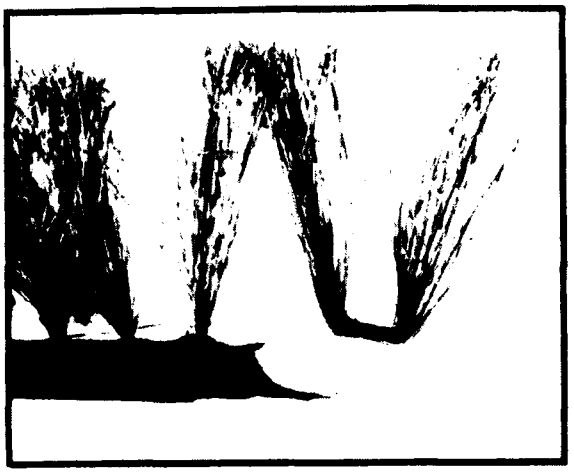

FRINGE

BRISTLE (TOP) AND BRUSH

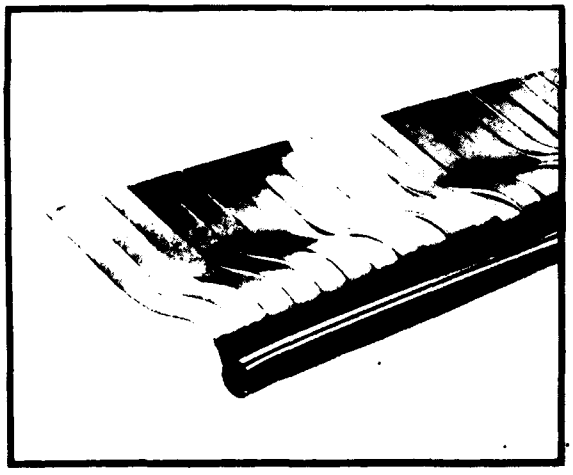

RIBBON

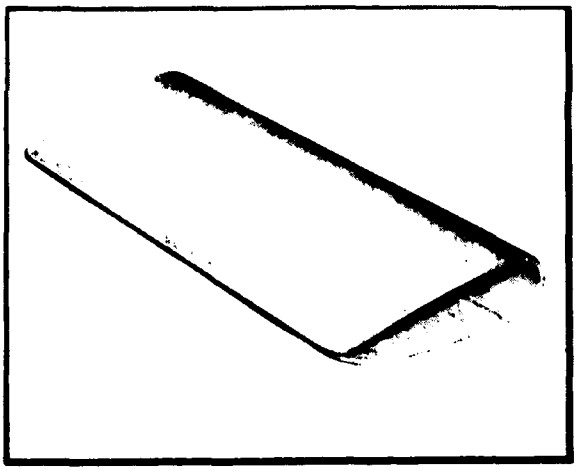

STREAMLINED, CLIP-ON TYPE

Figure 1. Various types of cable fairings

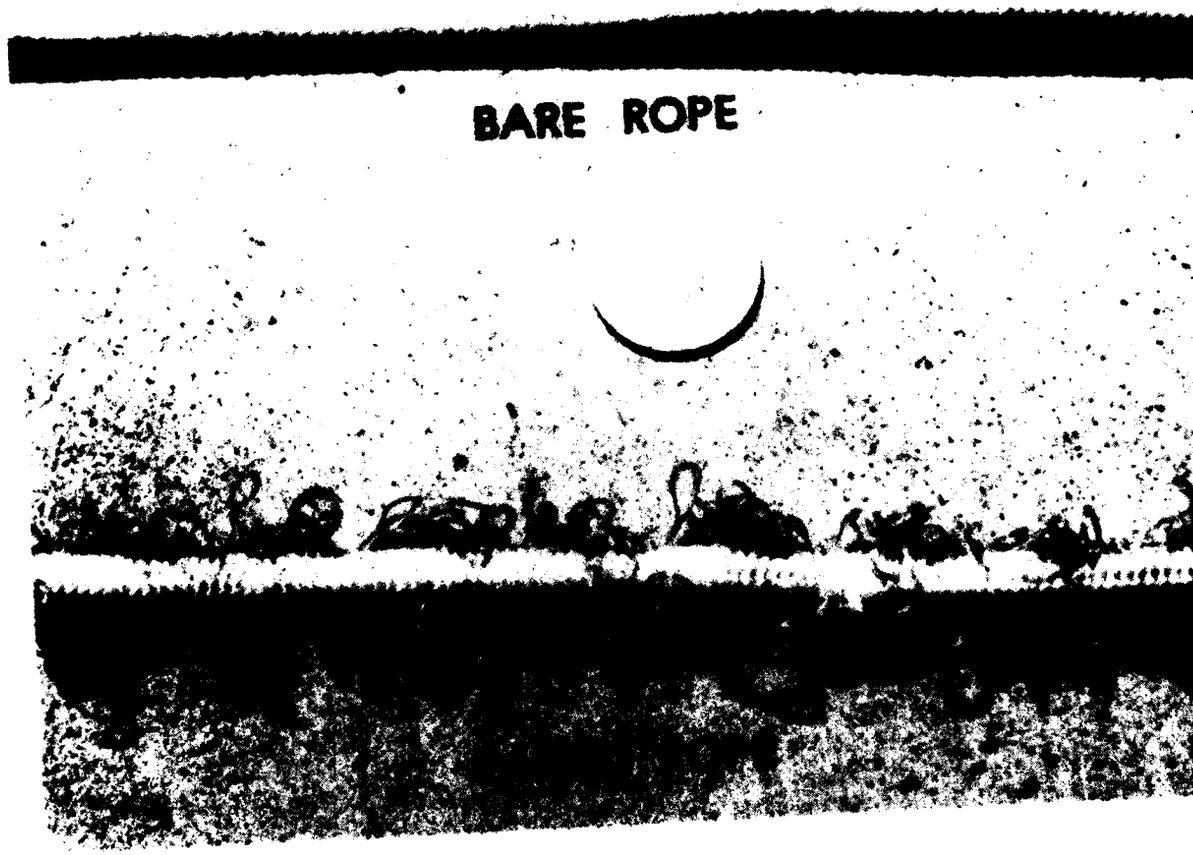

Figure 2. Photograph of Kevlar rope samples. Each rope has a 7.9 mm (5/16 inch) nominal diameter and consists of a Kevlar strength member covered with a tightly braided polyester jacket. The Kevlar yarns, comprising the strength member, are treated with a high pressure, water resistant wax to increase abrasion resistance. The fairing shown consists of loops of nylon yarn which are stitched to the rope jacket. The stitching runs continuously along the jacket on three nearly parallel lines about 120 degrees apart. Two of the three stitch lines can be seen in the photograph.

The rope samples were fabricated by Wall Industries, Inc. and are called Kevlar Miniline. Miniline is a registered trademark of Wall Industries, Inc., and Kevlar a registered tradename of E.I. DuPont de Nemours and Company.

F_t ds = tangential component of hydrodynamic force

V = relative flow speed, which acts opposite to the tow direction

ϕ = angle between tow direction and cable tangent vector

s = measure of distance along the cable

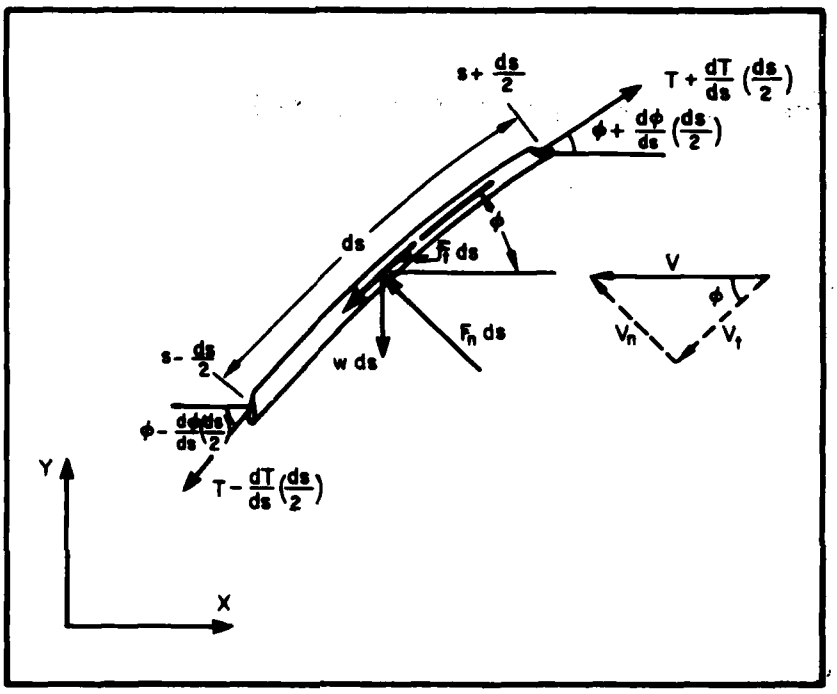

Figure 3. Free-body diagram of tow cable element

Based on the free-body diagram, the equilbrium equations which describe the steady-state behavior of the tow cable are

$$T \frac{d\phi}{ds} = -F_n + w \cos \phi \qquad (1)$$

and

$$\frac{dT}{ds} = F_t + w \sin \phi \qquad (2)$$

Equation (1) expresses the force balance normal to the cable element, and equation (2) the force balance tangential to the cable element.

The hydrodynamic forces that arise from the fluid flow are defined as

$$F_n \equiv 1/2\ \rho\ C_n\ d\ V_n^2 = 1/2\ \rho\ C_n\ d\ V^2 \sin^2 \phi \tag{3}$$

and

$$F_t \equiv 1/2\ \rho\ C_t\ \pi\ d\ V_t^2 = 1/2\ \rho\ C_t\ \pi\ d\ V^2 \cos^2 \phi \tag{4}$$

where ρ is the mass density of the fluid; d is the cable diameter; V_n is the flow speed normal to the cable and V_t is the flow speed tangential to the cable (See Figure 3); C_n is the normal drag coefficient of the cable; and C_t is the tangential drag coefficient of the cable, based on its wetted area. In this approach, the drag coefficients are considered as functions of the following velocity component Reynolds numbers, R_n and R_t:

$$C_n \alpha R_n \equiv \frac{d\ V \sin \phi}{\nu} \tag{5}$$

and

$$C_t \alpha R_t \equiv \frac{d\ V \cos \phi}{\nu} \tag{6}$$

where ν is the kinematic viscosity of the fluid. This simple treatment, which leads to a force model expressed as a function of cable angle, has been found to be in good agreement with experimental data for round cables (Casarella and Parsons, 1970).

When a uniform cable is towed without any attached bodies, its configuration is a straight line, inclined at an angle ϕ_c to the flow. This angle is called the critical angle by Pode (1951) and does not vary along the cable. Thus, $d\phi/ds = 0$ and equation (1) becomes

$$-1/2\ \rho\ C_n\ d\ V^2 \sin^2 \phi_c + w \cos \phi_c = 0 \tag{7}$$

after using equation (3). Furthermore, after using equation (4) and integrating the result from s = 0 to L, equation (2) becomes

$$T_1 = \left[1/2\ \rho\ \pi\ d\ C_t\ V^2 \cos^2 \phi_c + w \sin \phi_c\right] L \tag{8}$$

where L is the cable length and T_1 is the cable tension at the tow point s = L.

It is clear that the critical angle is the root of equation (7) which is quadratic in cos ϕ_c since $\sin^2\phi_c = 1 - \cos^2\phi_c$. Hence, its admissible solution is given by

$$\cos \phi_c = - \frac{w}{2R^*} + \sqrt{(\frac{w}{2R^*})^2 + 1} \tag{9}$$

where $R^* = 1/2 \rho C_n d V^2$. From this, it can be seen that ϕ_c varies from 90° at zero speed to 0° at infinite speed, in a manner depending on the cable characteristics: w, d, and C_n.

To examine how R_n varies, combine equations (5) and (7). This gives

$$R_n = \frac{1}{\nu} \sqrt{\frac{2 w d \cos \phi_c}{\rho C_n}} \tag{10}$$

and shows that the range of Reynolds numbers, over which C_n can be determined, is limited by the cable characteristics.

Equations (7) and (8) can also be rearranged to yield the relations on which the cable drag experiments are based. These are

$$C_n = (w \cos \phi_c) / (1/2 \rho d V^2 \sin^2 \phi_c) \tag{11}$$

and

$$C_t = T^*(1 - \frac{w \sin \phi_c}{T^*}) / (1/2 \rho \pi d V^2 \cos^2 \phi_c) \tag{12}$$

where $T^* = T_1/L$. Thus, for any non-zero tow speed, an experimental measure of ϕ_c will provide a value of C_n and an experimental measure of ϕ_c and T_1 a value of C_t.

B. SENSITIVITY ANALYSIS

Because of experimental conditions and instrumentation, however, the measured quantities in equations (11) and (12) will be in error. And this, in turn, will lead to errors in the computed values of C_n and C_t. To examine this effect, differentiate equations (11) and (12) while holding as constant ρ, d, and L (which can be very accurately measured). Next, divide the variational equation for C_n by C_n and the variational equation for C_t by C_t. The resulting sensitivity relations are then

$$\frac{\Delta C_n}{C_n} = \frac{\Delta w}{w} - 2\,\frac{\Delta V}{V} - \alpha_1\,\Delta\phi_c \tag{13}$$

and

$$\frac{\Delta C_t}{C_t} = \alpha_2 \frac{\Delta T_1}{T_1} + \alpha_3\,\frac{\Delta w}{w} - 2\,\frac{\Delta V}{V} - \alpha_4\,\Delta\phi_c \tag{14}$$

where Δ is the variational symbol and

$$\alpha_1 = \frac{2 + \tan^2\phi_c}{\tan\,\phi_c} \tag{15a}$$

$$\alpha_2 = 1/(1 - w \sin\,\phi_c/T^*) \tag{15b}$$

$$\alpha_3 = \alpha_2\,(w \sin\,\phi_c/T^*) \tag{15c}$$

$$\alpha_4 = -2 \tan\,\phi_c + \alpha_2\,\frac{w}{T^*}\cos\,\phi_c \tag{15d}$$

From an examination of equation (15a), it is found that α_1 has an absolute minimum of $2\sqrt{2}$ which occurs at $\phi_c = \tan^{-1}\sqrt{2} \simeq 54.7^\circ$. This can be seen in Figure 4 where α_1 is plotted versus ϕ_c for values of α_1 up to 10. Since α_1 increases monotonically from $2\sqrt{2}$ to $+\infty$ at $\phi_c = 0^\circ$ and 90°, it is therefore apparent that even if $\Delta W = \Delta V = 0$ the relative error in the C_n calculations can become quite large at relatively steep and shallow towing angles.

The coefficients α_2, α_3 and α_4 can be more easily examined by using equations (7) and (8) in equations (15b-d). This gives

$$\alpha_2 = 1 + \gamma\tan^3\phi_c = 1 + \alpha_3 \tag{16a}$$

$$\alpha_3 = \gamma\,\tan^3\,\phi_c \tag{16b}$$

$$\alpha_4 = \tan\,\phi_c\,(\gamma\,\tan\,\phi_c - 2) \tag{16c}$$

where $\gamma = C_n/(\pi\,C_t)$. From these equations, it is clear that the values of the coefficients decrease rapidly from $+\infty$ at $\phi_c = 90^\circ$ to $\alpha_2 = 1$ and $\alpha_3 = \alpha_4 = 0$ at $\phi_c = 0^\circ$. Further examination of equation (16c) reveals that α_4 has a root at $\phi_c = \tan^{-1}\,(2/\gamma)$ and an absolute minimum of $-1/\gamma$ at $\phi_c = \tan^{-1}\,(1/\gamma)$.

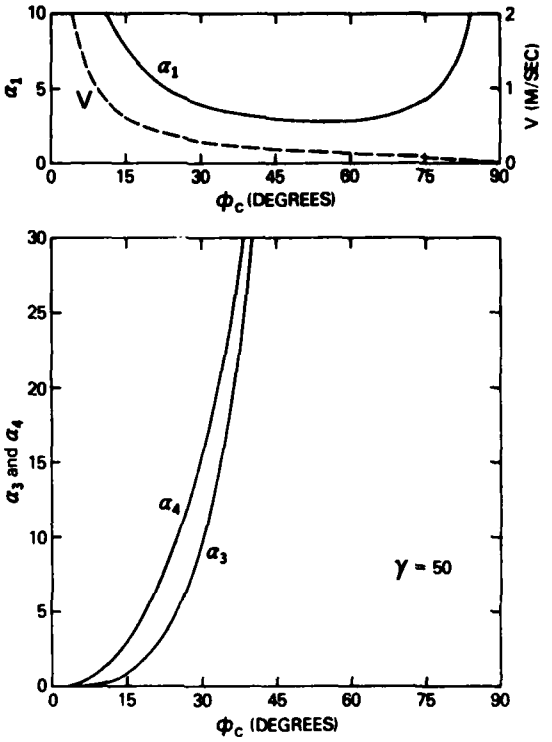

Figure 4. Sensitivity relation coefficients versus towing angle. The dash-line curve was computed from equation (7) using ρ = 1000 kg/m^3, d = 7.9 mm, w = 0.15 N/m and C_n = 1.4.

Wilson (1960) gives plots of C_n and C_t data as functions of Reynolds number for different types of round cables. From this data, it is found that values of γ typically range from 25 to 70. In Figure 4, α_3 and α_4 are plotted as functions of cable angle for γ = 50 which is considered to be a good approximation for the Kevlar ropes. Although the choice of γ remains a question, however, it is clear from Figure 4 that relative errors in the C_t calculations are smallest at shallow towing angles, or high speeds.

For sufficiently high speeds, ϕ_c will become small enough so that $\cos \phi_c \simeq 1$ and $\tan \phi_c \simeq \phi_c$. Hence, from equations (15b) and (16a) it is found that

$$1 - \frac{w \sin \phi_c}{T^*} \simeq \frac{1}{1 + \phi_c^3} \simeq 1$$

which on substitution into equation (12) yields

$$C_t \simeq T^*/(1/2\ \rho\ \pi\ d\ V^2) \qquad (17)$$

And for these values of C_t, the corresponding Reynolds numbers can be computed as

$$R_t = \frac{V\, d \cos \phi_c}{\nu} \simeq \frac{V\, d}{\nu} \qquad (18)$$

C. EXPERIMENTAL SETUP AND PROCEDURES

Based on the sensitivity analysis, two experiments were conducted: One (called the tangential drag experiment) to determine values of C_t as a function of R_t, the other (called the normal drag experiment) to determine values of C_n as a function of R_n. Both are illustrated in Figure 5.

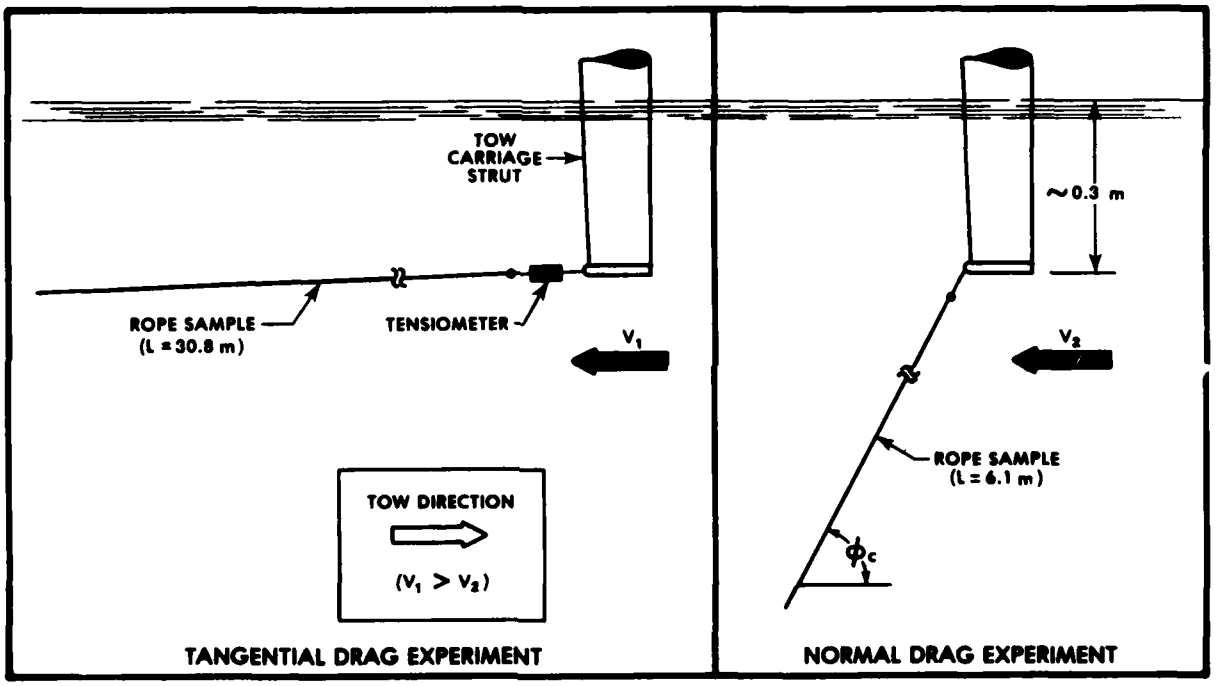

Figure 5. Schematic of experimental setup for cable drag measurements

In the tangential drag experiment, each 30.8 m long sample was freely towed at constant speeds of 0.515 m/s (1.00 knots) to 2.575 m/s (5.00 knots) in increments of 0.515 m/s. For each speed (or run), the voltage output from the tensiometer shown in Figure 5 was recorded. Three sets of runs were made for each sample.

After completing this experiment, each sample was cut to obtain a 6.1 m long piece. These shorter length samples, required to prevent dragging on the bottom, were then freely towed at constant speeds of 0.129 m/s (0.25 knots) to 0.515 m/s in increments of 0.129 m/s. This series of runs comprised the normal drag experiment. To obtain a measure of towing angle, the towed samples were photographed through an observation window located in the wall of the tow basin.

The towing speeds selected for the experiments were intended to yield the optimum towing angles for computing drag coefficients. This can be seen in Figure 4 where tow speed is plotted against towing angle for a cable having the same nominal characteristics as that of the bare Kevlar rope.

For each experiment, the rope samples were secured to the towing strut with a piece of string. Since this would allow the rope sample to rotate, the orientation of the fairing to the flow of water is not known. The tow point on the strut was submerged about 0.3 m below the water surface to minimize boundary effects. Speed of the tow carriage was also adjusted to within ± 0.5 cm/s of that desired, and water temperature was measured to determine values of ρ and ν. Before conducting either experiment, the rope samples were thoroughly soaked to insure a stable in-water weight.

The diameter, length, and weight (in air and water) of each rope sample was accurately measured after completing the experiments. Because entrapped air was a potential source of error, each rope sample was weighed while wet at predetermined time intervals. After their weights had stabilized, the samples were removed and allowed to dry. This procedure was repeated three times to obtain an error estimate (ΔW) based on the standard deviation of the measurements.

D. MEASUREMENTS AND OBSERVATIONS

While conducting the drag experiments, no appreciable (if any), rope vibration was observed. Each sample also appeared to tow in the vertical plane defined by the directions of gravity and tow. Figure 6, which is composed of the photographs that were taken, shows the in-plane shape of each sample while towed in the normal drag experiment. It does not include, however, a photograph of the bare rope sample towed at 0.129 m/s since the rope dragged on the bottom of the tow basin during this run.

In measuring values of ϕ_c from the photographs, the bare rope was found to fit a straight line reasonably well for each tow speed. Except for 0.515 m/s, this highly satisfactory agreement with theory was not found for the faired rope sample however. Instead, the shape of the faired rope was found to be best fit by two straight line segments at the three lowest tow speeds. This effect can be seen in Figure 6, and is possibly caused by a nonuniform orientation of the fairing to the flow. If so, then C_n and hence cable angle would vary along the rope.

In spite of the cause, however, the effect was reduced significantly at the highest tow speed. This might be expected since equation (1) shows that angular changes are inversely proportional to tensions which increase with tow speed.

Table 1 gives the measured characteristics of the rope samples, and Table 2 the measured values of ϕ_c and T_1/L. The quantities given are mean values of the measurements, and are used to calculate the drag coefficients and associated Reynolds numbers. The fluid characteristics used in these calculations are $\rho = 997.9\ kg/m^3$ and $\nu = 0.9798 \times 10^{-6}\ m^2/s$. They are based on a measured tow basin water temperature of 21°C.

Because of its bilinear tow shape, Table 2 gives two values of towing angle for the faired rope at the three lowest speeds. A drag coefficient is calculated for each value. Hence, in this approach, each line segment is treated as a freely towed rope with a constant value of C_n.

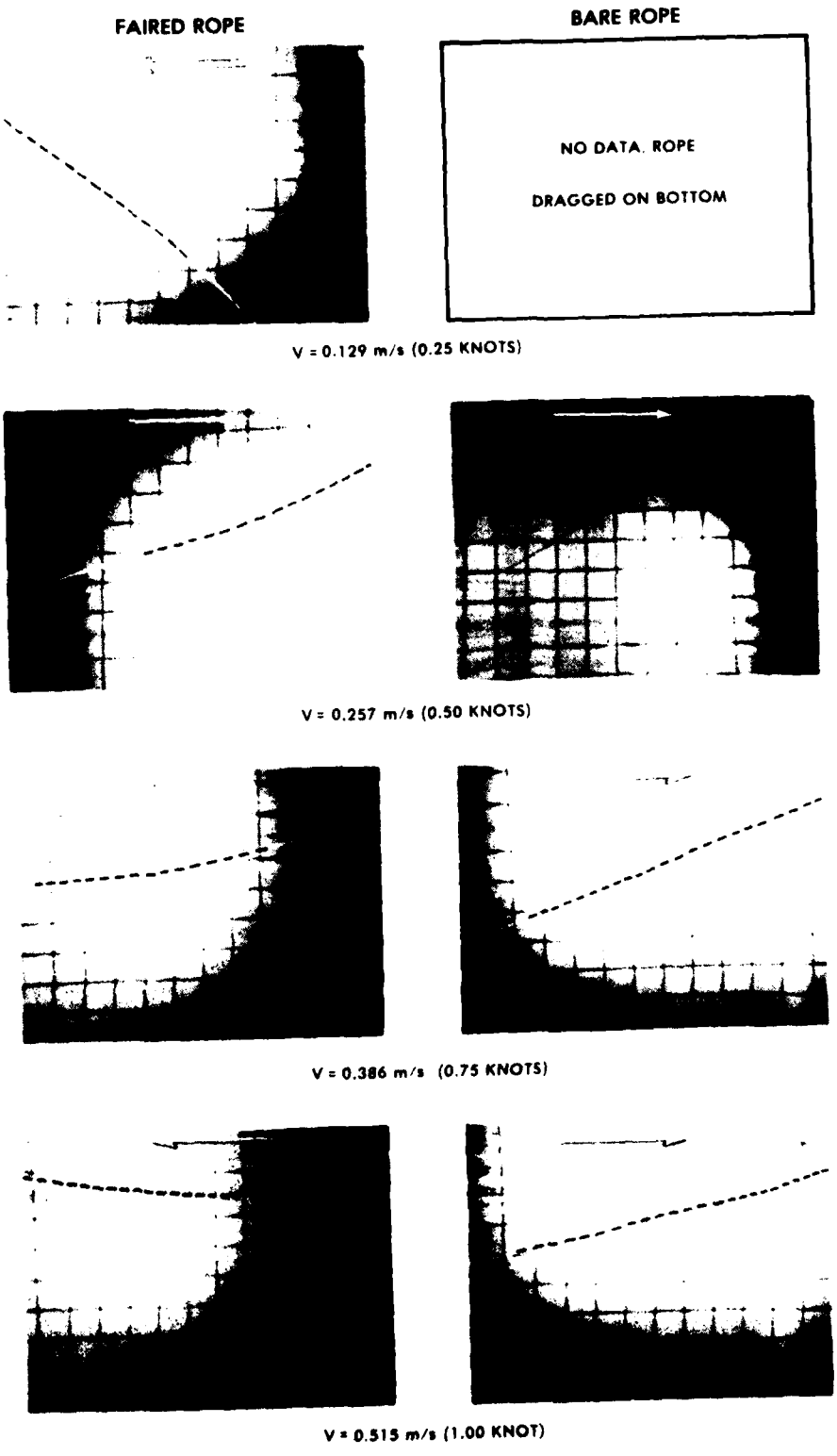

Figure 6. Photographs of 6.1 m long rope samples towed freely at various speeds. Dotted lines accent the cable.

Table 1

Measured Rope Sample Characteristics

Characteristic	Bare rope	Faired rope
Diameter, mm	8.3	7.8
Weight in water, N/m	0.108	0.098
Mass, kg/m	0.055	0.050
Length, m		
• Normal drag experiment	6.1	6.1
• Tangential drag experiment	30.8	30.8

Table 2

Cable Drag Measurements[a]

Experiment	Tow speed, V (m/s)	Bare Rope		Faired rope	
		ϕ_c (degrees)	T_1/L (N/m)	ϕ_c (degrees)	T_1/L (N/m)
Normal drag (L = 6.1m)	0.129	-	-	36 & 45[b]	-
	0.257	29	-	22 & 17[b]	-
	0.386	21	-	13 & 6[b]	-
	0.515	14	-	7	-
Tangential drag (L = 30.8 m)	0.515	-	0.058	-	0.260
	1.030	-	0.108	-	0.693
	1.545	-	0.253	-	1.256
	2.060	-	0.448	-	2.022
	2.575	-	0.679	-	2.874

[a] A parameter not measured is indicated by a dashed line.

[b] Towed rope shape best described by two straight lines that have the critical angles given.

The variations found in the measured quantities were also used in the calculations of drag coefficients and Reynolds numbers. They are

$$\Delta L = \Delta d = \Delta \rho = 0$$

$$\Delta w = \pm 0.05\ w$$

$$\Delta \phi_c = \pm 1^\circ$$

$$\Delta V = \pm 0.5\ \text{cm/s}$$

$$\Delta T_1 = \pm (0.01\ T_1 + 0.445\ \text{N})$$

$$\Delta \nu = \pm 0.2450 \times 10^{-7}\ \text{m}^2/\text{s}$$

where ΔT_1 is in newtons and the variation in ν is based on a $\pm$1°C temperature error. The results of such an analysis yield high and low values, obtained in the usual fashion.

The computed values of C_n and R_n are given in Table 3, and the computed values of C_t and R_t in Table 4. Values of C_n are based on equation (11), and values of R_n on equation (5). Equations (6) and (12) were used to calculate values of C_t and R_t for the bare and faired ropes towed at 0.515 m/s and for the bare rope towed at 1.030 m/s. The towing angles used for the 0.515 m/s speed are those obtained from the normal drag experiment, and the towing angle for the bare rope towed at 1.030 m/s is conservatively based on a normal drag coefficient value of 1.4. The remaining C_t and R_t values given were computed from equations (17) and (18) which were found to be reasonably valid.

Table 3

Normal Drag Coefficient and Reynolds Number as a Function of Tow Speed

Tow speed, V (m/s)	Normal drag coefficient, C_n		Reynolds number, R_n	
	Mean value	Range of values	Mean value	Range of values
Bare rope				
0.129	--	--	--	--
0.257	1.47	1.24 - 1.75	1057	969 - 1152
0.386	1.28	1.06 - 1.54	1172	1066 - 1287
0.515	1.64	1.31 - 2.06	1055	938 - 1181
Faired rope				
0.129	2.15	1.77 - 2.60	726	661 - 796
	3.55	2.91 - 4.35	604	546 - 666
0.257	2.51	2.07 - 3.04	769	697 - 848
	3.78	3.06 - 4.69	635	568 - 707
0.386	3.25	2.56 - 4.16	693	610 - 782
	15.3	10.3 - 24.1	322	256 - 394
0.515	6.34	4.47 - 9.34	501	411 - 598

Table 4

Tangential Drag Coefficient and Reynolds Number as a Function of Tow Speed

Tow speed,V (m/s)	Tangential drag Coefficient, C_t		Reynolds number, R_t	
	Mean Value	Range of values	Mean value	Range of values
Bare rope				
0.515	0.0098	0.0040 - 0.0160	4232	4029 - 4447
1.030	0.0070	0.0055 - 0.0085	8653	8296 - 9028
1.545	0.0082	0.0074 - 0.0090	13086	12513 - 13692
2.060	0.0081	0.0076 - 0.0087	17448	16684 - 18255
2.575	0.0079	0.0074 - 0.0084	21810	20855 - 22819
Faired rope				
0.515	0.0803	0.0729 - 0.0882	4108	3928 - 4298
1.030	0.0536	0.0504 - 0.0569	8216	7856 - 8596
1.545	0.0431	0.0410 - 0.0454	12324	11784 - 12894
2.060	0.0390	0.0373 - 0.0409	16431	15712 - 17191
2.575	0.0355	0.0340 - 0.0372	20539	19639 - 21489

E. DRAG COEFFICIENT COMPARISONS

In Figure 7, the normal drag coefficient data are plotted against the Reynolds number data for the Kevlar rope samples and for other types of cables as well. The solid line curve shown is an experimentally derived relationship for a smooth circular cylinder. But the bare rope is not smooth since its woven jacket has fairly uniformly distributed surface inequalities. It is therefore not surprising to find that its data lies above the solid line. Although there appears to be a dependence on R_n, the centroid of the three data points for the bare rope suggests a C_n value of 1.5 within the Reynolds number range of about 950 to 1300. And this is seen to be in reasonable accord with the test data found for stranded cables, the dashed-line curve in Figure 7.

The C_n data for the faired rope shows a negative gradient somewhat similar to the Vandiver and Pham (1977) data shown in Figure 7. The Vandiver and Pham data apply to the fringe fairing shown in Figure 1, and show that flow into the fairing increases C_n by about 70% over those cases when the fairing is oriented downstream. An examination of the Table 3 data shows that the two C_n values of the faired rope sample at speeds of 0.129 and 0.257 m/s differ by about 50%.

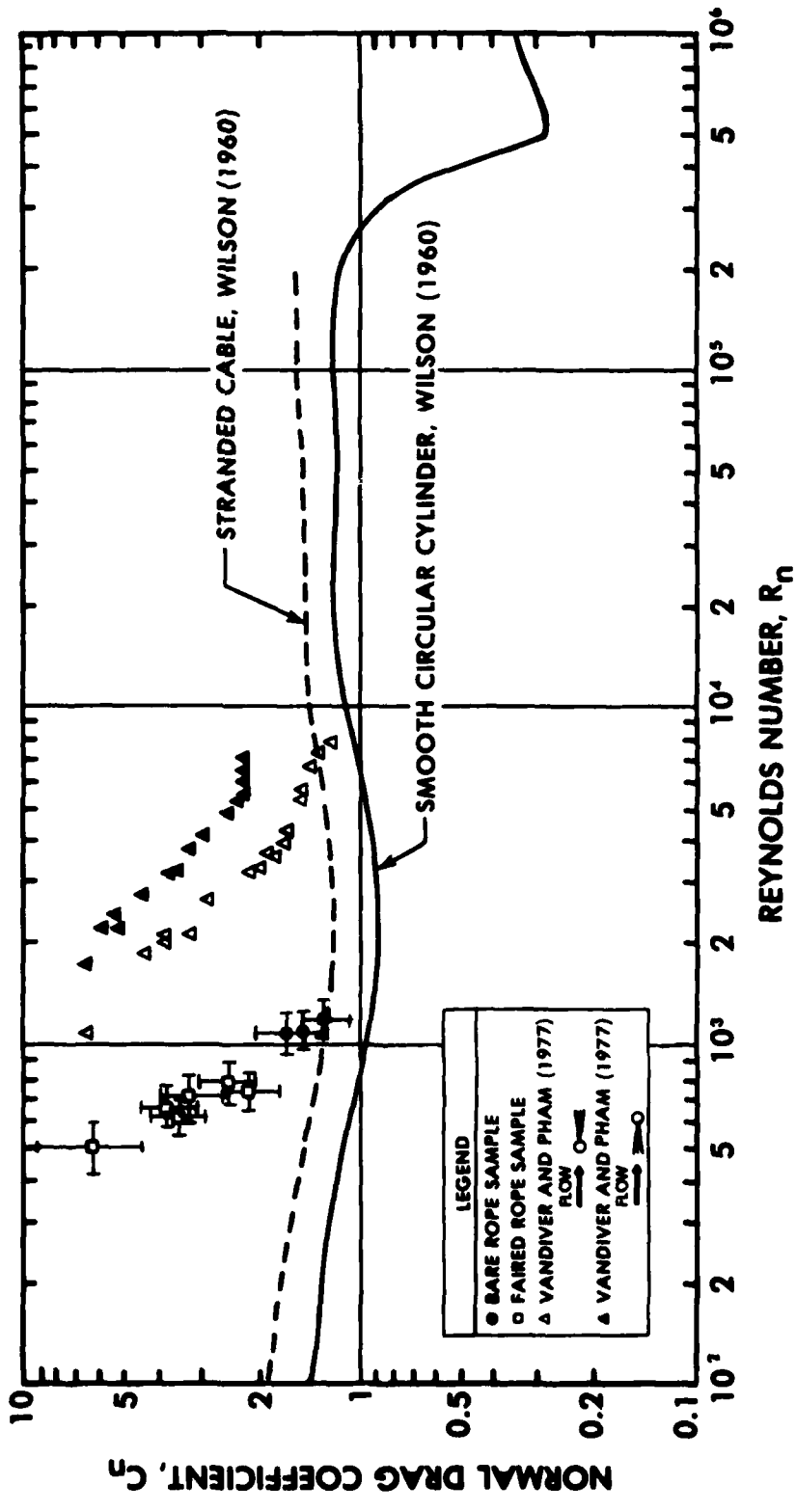

Figure 7. Normal drag coefficients versus Reynolds number

The centroid of the faired rope data suggests $C_n = 3.6$ for Reynolds numbers between 550 to 850. This increase is nearly 250% over that of the bare rope. Such a comparison, however, does not consider the effect of increased drag as a result of vortex-excited cable oscillations. In particular, the Griffin et al. (1981) survey of cable strumming experiments shows that the normal drag coefficient of a vibrating bare cable can be increased by as much as 150 to 300%. Hence, if the fairing impedes or even substantially lessens strumming, the drag coefficient of the vibrating bare rope can approach that of the faired rope.

The C_t data for the bare and faired rope samples are plotted versus Reynolds number in Figure 8. In this figure, theoretically derived curves for a smooth and a rough circular cylinder are also shown for purposes of comparison. It can be seen that the bare rope data lie between the two curves, as expected.

The C_t data for the faired rope exhibit a dependence on Reynolds number, which is probably caused by the fairing. This same type of dependence is not apparent for the bare rope data which have C_t values that vary between 0.007 and 0.009. It is noteworthy that these values are in reasonable agreement with the stranded cable data studied by Wilson (1960), who found a most probable C_t value of 0.008 to 0.01. Finally, it can be seen that C_t values for the faired rope are, depending on Reynolds number, about 4 to 10 times greater than those found for the bare rope.

III. STRUMMING EXPERIMENT

A. VIBRATION THEORY FOR TAUT CABLES

Vortices shed coherently from a cable will produce transverse cable vibrations at the vortex shedding frequency f_s. For a stationary cylinder or cable

$$f_s = S\ V/d \tag{19}$$

where S is the Strouhal number and V is the velocity of fluid normal to the cylinder. For Reynolds numbers between 400 and 10^5, values of S vary from 0.20 to 0.22 (Griffin et al., 1981).

If the vortex shedding frequency coincides with the natural frequency of the cable, then vibration amplitudes will reach peak values. Experimental studies have shown that the natural frequencies f_k of a taut cable are reasonably estimated from the classical string relation

$$f_k = (k/2L)\ (T_1/M)^{1/2} \tag{20}$$

where k is the vibration mode number, T_1 is the static cable tension, and M is the virtual mass of the cable (mass plus added mass). The flow speeds which might produce resonance can therefore be found by equating equations (19) and (20) and solving for V.

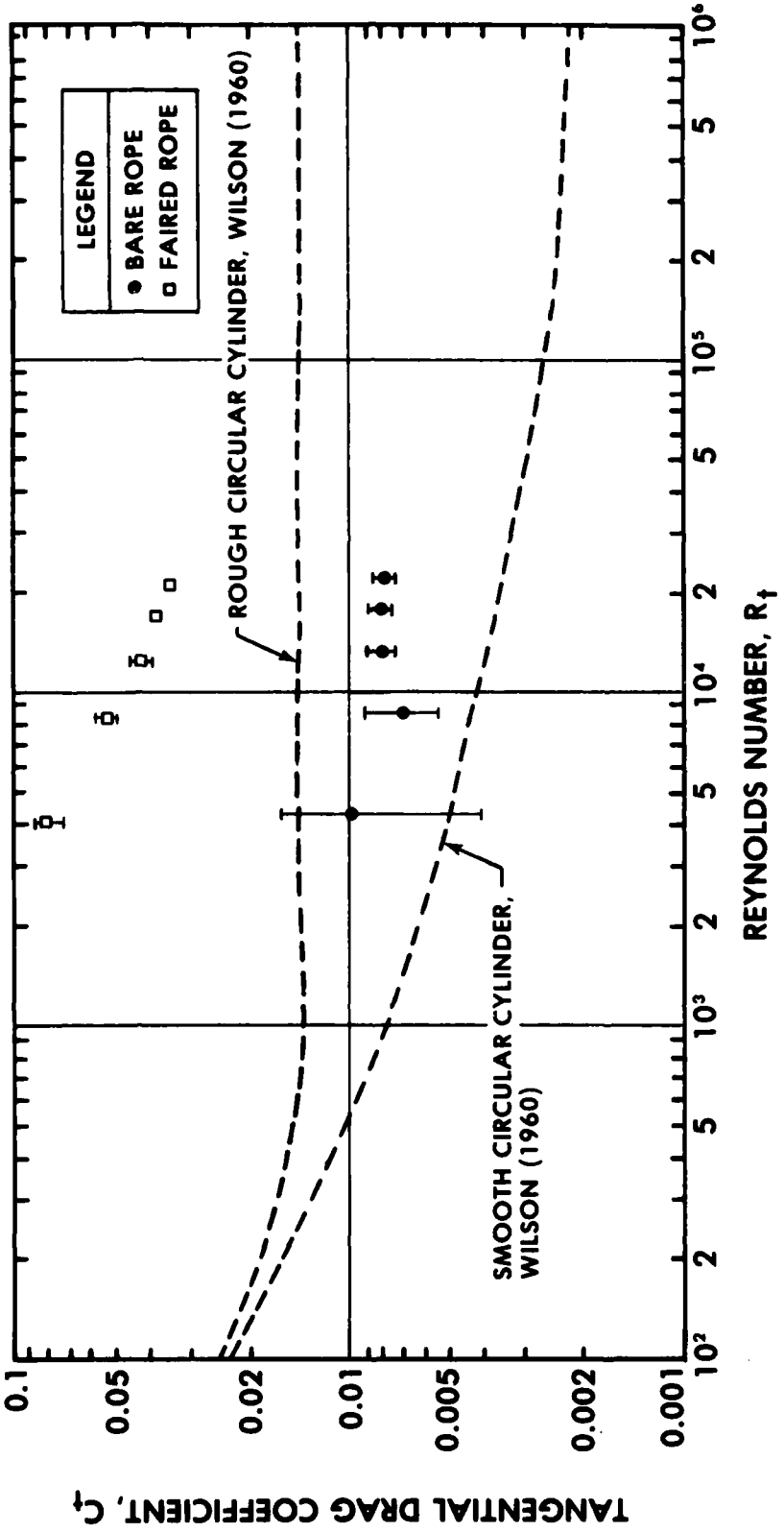

Figure 8. Tangential drag coefficients versus Reynolds number

The tension fluctuations T_f occurring at the ends of a resonantly vibrating, taut cable of length L are given by Griffin et al. (1981) as

$$T_f = \frac{3\pi^2 Y^2 k^2 EA}{2L^2} \sin^2 \omega t \qquad (21)$$

where Y is the transverse cable displacement at an antinode, EA is the cable's modulus of rigidity, ω is forcing frequency, and t is time. Hence, an evaluation of the strum suppression effectiveness of the yarn fairing may be obtained by comparing the resonantly excited tension amplitudes of the bare and faired rope samples. From equation (21), it is also clear that the fluctuating tensions occur at twice the cable vibration or forcing frequency.

B. EXPERIMENTAL SETUP AND PROCEDURES

The experimental arrangement used on each rope sample is illustrated in Figure 9. The body attached to the free end of the rope is used to tension the rope. It is streamlined to reduce drag and weighs about 400 N (90 lb) in water. Each rope sample was about 4.5 m long, a maximum based on the depth of the tow tank. The tensiometer was used to measure tension fluctuations at the tow point.

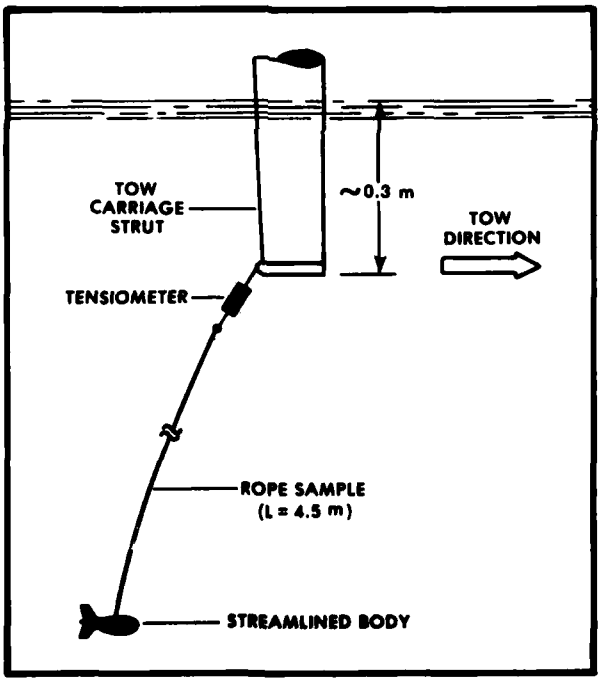

Figure 9. Schematic of experimental setup for cable strumming measurements

To obtain the measurements, the towing carriage was slowly accelerated from 0 to 2.6 m/s (5 knots) and then slowly decelerated to rest. During this run, tension fluctuations and carriage speeds were simultaneously and continuously recorded on a strip chart recorder. Two sets of runs were made for each rope sample.

C. DISCUSSION OF RESULTS

Resonance started at about 0.1 m/s for both rope samples. At about 0.2 m/s, tension amplitudes in both reached peak values: About 12 N for the bare rope and 4 N for the faired rope. The tension fluctuations in both were nearly sinusoidal with about a 9 Hz frequency, which indicates a resonant lock-in phenomenon. Based on equation (21), this suggests a strumming frequency of about 4-1/2 Hz and about a 40% reduction in strumming amplitude for the faired rope.

As speed was increased from 0.2 to 1.6 m/s, the bare rope responded at three higher resonant cable vibration modes: The second mode with a 14 Hz strumming frequency at about 0.8 m/s; the third mode with a 19-1/2 Hz strumming frequency at about 1.1 m/s; and, the fourth mode with a 27 Hz strumming frequency at about 1.6 m/s. The tension fluctuations for these modes were not as steady as those found for the first mode. This can be seen in Figure 10 where selected tension fluctuation data are shown. At speeds above 1.6 m/s, the tension fluctuations and frequencies of the bare rope were severe, indicating that the natural vortex shedding frequency is outside the wake synchronization range.

In contrast, the faired rope did not respond resonantly at any of the higher cable vibration modes. Instead, at speeds above 0.2 m/s, its tension fluctuations were irregular and much less severe than those of the bare rope (see Fig. 10). It is conjectured that the fairing increases damping and disrupts the spatial coherence of the vortices. If so, then wake synchronization and strumming would be suppressed.

The resonant vibration characteristics of the bare rope are plotted as a function of flow speed and Reynolds number in Figure 11. Reynolds number calculations neglect the effect of flow angle since it is assumed that for speeds up to 1.6 m/s angular deflections from the vertical are small. The model of Dale et al. (1966) is empirically derived from test data obtained by towing cables with a body attached to its free end. It assumes a larger virtual cable diameter for the strumming cable and, hence, it is not surprising to find that it predicts the frequency response better than that of equation (19). The agreement between the predicted and the experimentally observed natural frequencies is generally satisfactory, except for the fundamental mode. In calculating the natural frequencies, a theoretical added mass coefficient of 1 was used which is a major source of error in the calculations.

IV. CONCLUSIONS

Based on the experimental results, the following conclusions can be made:

- The tangential drag coefficient of the faired rope is, depending on Reynolds number, about 4 to 10 times greater than that found for the bare rope.
- For Reynolds number between 550 to 850, the faired rope has an average normal drag coefficient of 3.6 which represents an increase of nearly 250 percent over that of a non-strumming bare rope.
- Although the experimental method used to determine normal drag coefficients is simple and economical, it is highly unreliable due principally to errors in the cable angle measurements.
- The yarn fairing is an inexpensive and effective method of reducing strumming in Kevlar ropes and cables.

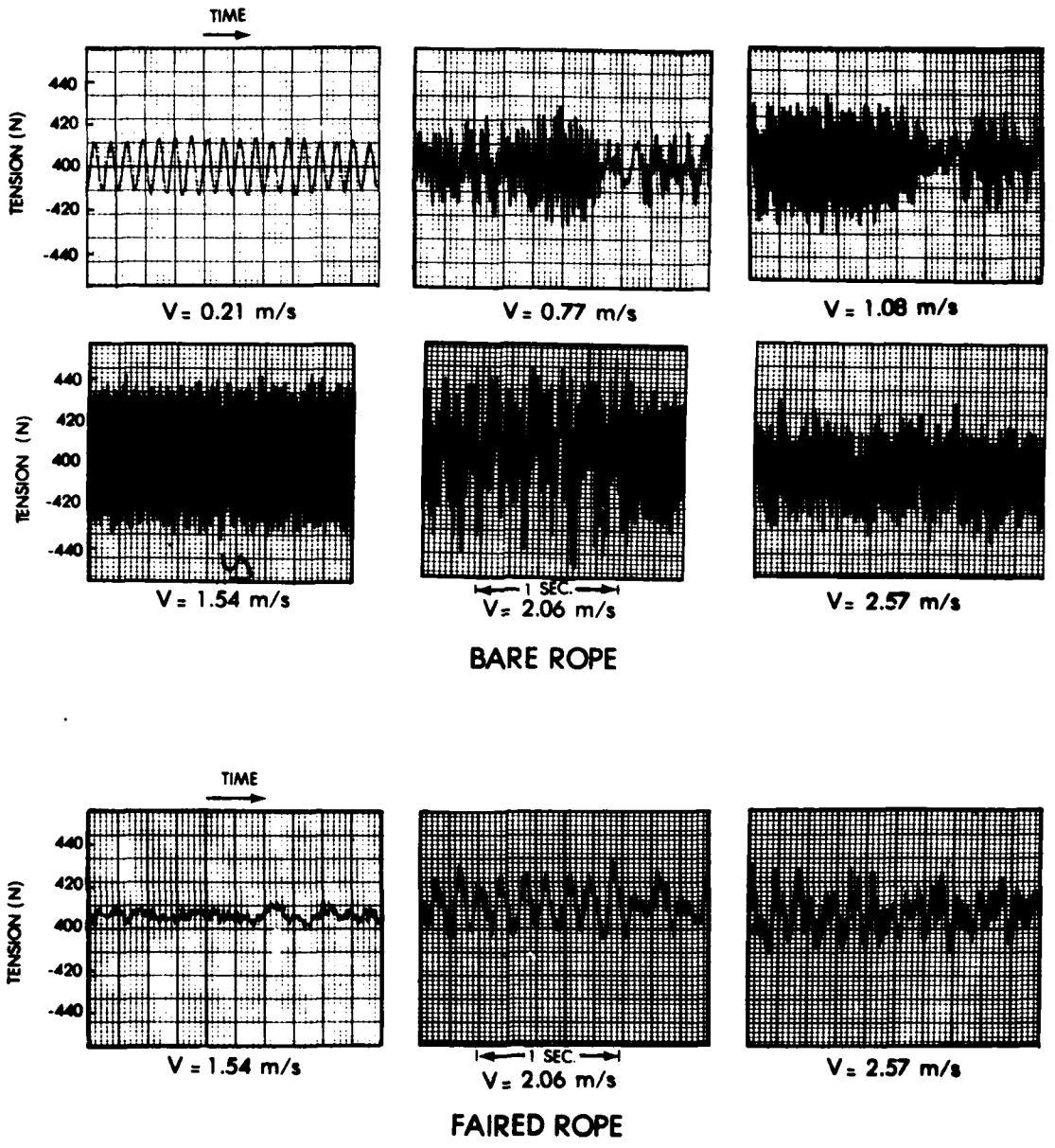

Figure 10. Tension fluctuation data for the rope samples. For speeds between 0.2 and 1.3 m/s, the peak value of the tension fluctuations in the faired rope rarely exceeded 2 N.

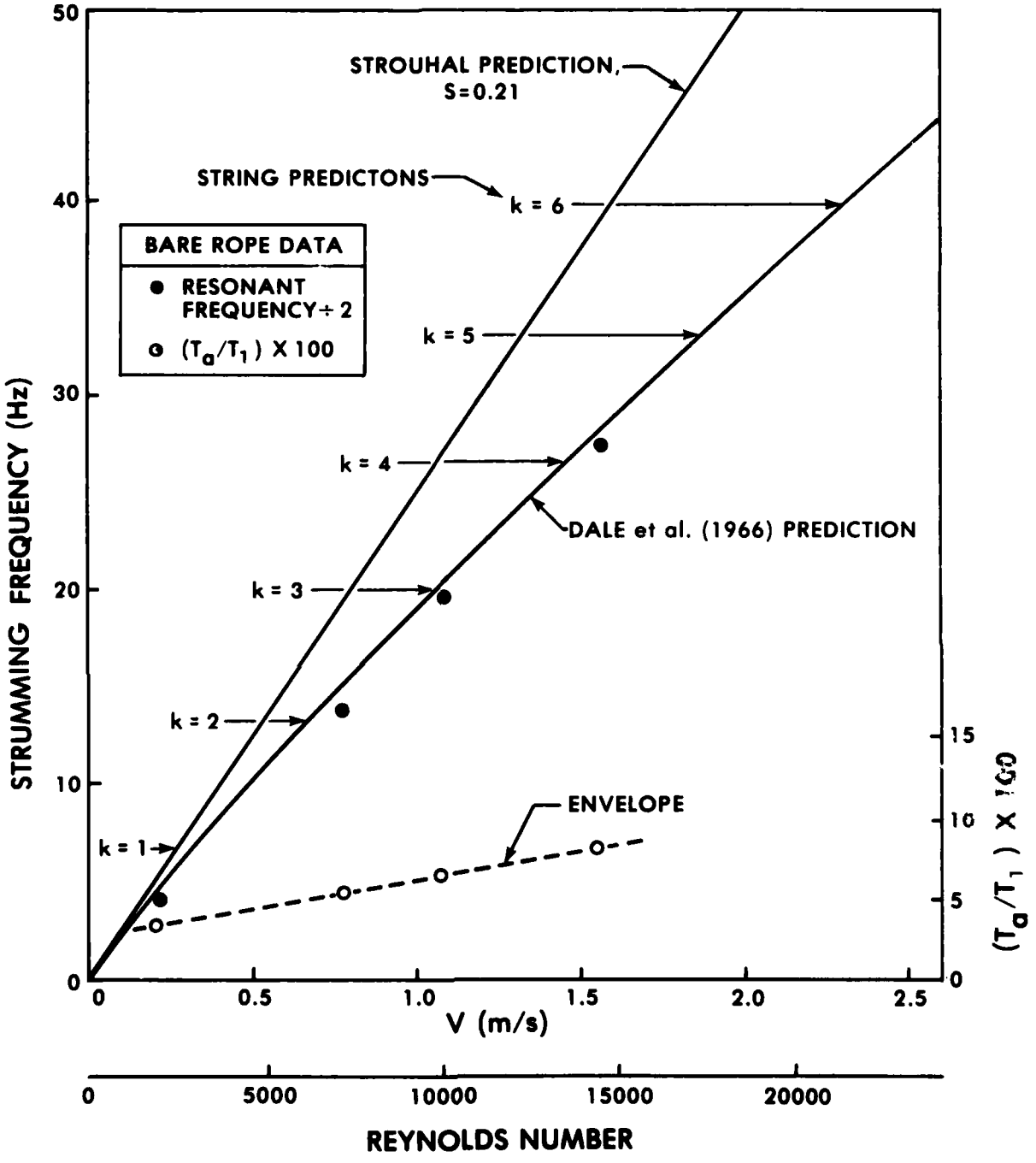

Figure 11. Vibration characteristics of the bare rope sample. The tension amplitude response is shown by the hollow circles where T_a is the amplitude of the tension fluctuations.

V. REFERENCES

Casarella, M. J. and M. G. Parsons (1970). A Survey of Investigations on the Configuration and Motion of Cable Systems Under Hydrodynamic Loading. MTS J., v. 4, July-Aug., p. 27-44.

Dale, J. et al. (1966). Dynamic Characteristics of Underwater Cables Flow Induced Transverse Vibrations. U. S. Naval Air Development Center, Johnsville, PA, Sept., Rpt. No. NADC-AE-6620.

Griffin, O. M. et al. (1981). The Strumming Vibrations of Marine Cables: State of the Art. Civil Engineering Laboratory, Port Hueneme, CA, May, Tech. Note N-1608, 179 p.

Pode, L. (1951). Tables for Computing the Equilibrium Configuration of a Flexible Cable in a Uniform Stream. David W. Taylor Naval Ship Research and Development Center, Carderock, MD, Mar., Report 687, 223 p.

Rispin, P. et al. (1977). An Evaluation of Several Techniques for Reducing Cable Strum. David W. Taylor Naval Ship Research and Development Center, Carderock, MD, Nov., Report SPD 732-01, 57 p.

Vandiver, J. K. and T. Q. Pham (1977). Performance Evaluation of Various Strumming Suppression Devices. Massachusetts Institute of Technology, Cambridge, MA, Mar., Rpt. No. 77-2, 105 p.

Wilson, B. W. (1960). Characteristics of Anchor Cables in Uniform Ocean Currents. Texas A&M University, College Station, TX, Apr., Tech. Rpt. No. 204-1, 157 p.

UNCLASSIFIED

SECURITY CLASSIFICATION OF THIS PAGE *(When Data Entered)*

REPORT DOCUMENTATION PAGE	READ INSTRUCTIONS BEFORE COMPLETING FORM
1. REPORT NUMBER NORDA Technical Note 118	2. GOVT ACCESSION NO. AD A113 478	3. RECIPIENT'S CATALOG NUMBER
4. TITLE *(and Subtitle)* Hydrodynamic Test and Evaluation of a Newly Developed Kevlar Rope Fairing		5. TYPE OF REPORT & PERIOD COVERED 6. PERFORMING ORG. REPORT NUMBER
7. AUTHOR(s) Darrell A. Milburn Paul Rispin		8. CONTRACT OR GRANT NUMBER(s)
9. PERFORMING ORGANIZATION NAME AND ADDRESS Naval Ocean Research and Development Activity Code 351 NSTL Station, Mississippi 39529		10. PROGRAM ELEMENT, PROJECT, TASK AREA & WORK UNIT NUMBERS
11. CONTROLLING OFFICE NAME AND ADDRESS Naval Ocean Research and Development Activity Code 351 NSTL Station, Mississippi 39529		12. REPORT DATE February 1982 13. NUMBER OF PAGES 27
14. MONITORING AGENCY NAME & ADDRESS*(if different from Controlling Office)*		15. SECURITY CLASS. *(of this report)* Unclassified 15a. DECLASSIFICATION/DOWNGRADING SCHEDULE

16. DISTRIBUTION STATEMENT *(of this Report)*

Distribution Unlimited

17. DISTRIBUTION STATEMENT *(of the abstract entered in Block 20, if different from Report)*

18. SUPPLEMENTARY NOTES

19. KEY WORDS *(Continue on reverse side if necessary and identify by block number)*

cable drag characteristics
cable strumming
cable strum reduction technique

20. ABSTRACT *(Continue on reverse side if necessary and identify by block number)*

The strumming and drag performance of a newly developed Kevlar rope fairing have been determined experimentally. In one experiment, faired and unfaired rope samples of the same diameter were towed with one end free to obtain their normal and tangential drag coefficients. Results of the experiment are plotted versus Reynolds number and show that the fairing increases cable drag substantially. In another experiment the same ropes were also towed with a heavy, streamlined body attached. By comparing their resonantly excited tension fluctuations, it is found that the fairing reduces flow-induced cable vibrations.

DD FORM 1 JAN 73 1473 EDITION OF 1 NOV 68 IS OBSOLETE
S/N 0102-LF-014-6601

UNCLASSIFIED

SECURITY CLASSIFICATION OF THIS PAGE *(When Data Entered)*